

**Synchronization versus neighborhood similarity in complex networks of nonidentical oscillators**Celso Freitas<sup>\*</sup> and Elbert Macau<sup>†</sup>*Associate Laboratory for Computing and Applied Mathematics—LAC,  
National Institute for Space Research—INPE, 12245-970, São José dos Campos, SP, Brazil*Ricardo Luiz Viana<sup>‡</sup>*Department of Physics, Federal University of Paraná—UFPR, 81531-990, Curitiba, PR, Brazil*

(Received 10 January 2015; published 2 September 2015)

Does the assignment order of a fixed collection of slightly distinct subsystems into given communication channels influence the overall ensemble behavior? We discuss this question in the context of complex networks of nonidentical interacting oscillators. Three types of connection configurations are considered: Similar, Dissimilar, and Neutral patterns. These different groups correspond, respectively, to oscillators alike, distinct, and indifferent relative to their neighbors. To construct such scenarios we define a vertex-weighted graph measure, the *total dissonance*, which comprises the sum of the dissonances between all neighbor oscillators in the network. Our numerical simulations show that the more homogeneous a network, the higher tend to be both the coupling strength required for phase locking and the associated final phase configuration spread over the circle. On the other hand, the initial spread of partial synchronization occurs faster for Similar patterns in comparison to Dissimilar ones, while neutral patterns are an intermediate situation between both extremes.

DOI: [10.1103/PhysRevE.92.032901](https://doi.org/10.1103/PhysRevE.92.032901)

PACS number(s): 05.45.Xt, 89.75.Fb

**I. INTRODUCTION**

Some social and biological studies about multiagents reveal that units tend to select similar peers with which to interact [1,2]. However, there are systems which behave in an opposite manner, where their components preferentially choose to connect themselves to others with some distinct inner characteristics [3]. In fact, nature seems to favor the former or the latter construction, which we respectively call *Similar* or *Dissimilar* (neighborhood) patterns, to achieve different agendas [4]. This article explores ideas inspired by these scenarios within the nonidentical-phase-oscillator Kuramoto model, which is one of the main paradigms to describe collective behavior and synchronization [5]. This model is also interesting because, under weak mutual interaction, it approximates dynamics of a large class of nonlinear oscillators near limit cycle [6]. Besides, this is an active research field with a number of applications from different areas [7–10], highlighting the fundamental role that synchronization plays.

Our numerical approach is based on a novel vertex-weighted graph measure: the *total dissonance*. This quantity can be regarded as a generalization of the classical concept of dissonance, that is, the natural frequency difference of two coupled oscillators [6]. So we define Similar and Dissimilar patterns as the assignments of nonidentical oscillators into the coupling graph which yield, respectively, significantly lower and higher total dissonance values. Otherwise, if a pattern has no strong bias related to this quantifier, then we call it *Neutral*. Given a fixed choice of inner properties for each oscillator and a fixed coupling graph, we search for Similar and Dissimilar patterns via an optimization algorithm interchanging oscillator's positions into the graph nodes.

Clearly, oscillator swapping over nodes of fully coupled networks have no influence over synchronization, since they can be solely seeing as an index reordering. We focus in this work on networks whose quantity of edges is much smaller than the all-to-all case. Regular, scale-free, random, small-world, and community networks are considered [11] to provide evidence about the ubiquity of our argument. Finally, massive numerical simulations are performed to grasp the influence of these three different neighborhood patterns over phase-synchronization quantifiers.

About related material, Refs. [12] and [13], respectively, explore first- and second-order Kuramoto model versions, both including local correlations between oscillator's natural frequency and node degree. They report an explosive synchronization in the first case and cascade synchronization, according to the node degree, in the second. Our methodology introduces a diverse relationship between natural frequencies and coupling graph, as will be discussed and illustrated in the text.

Optimization studies also have laid the foundation for our research. In Ref. [14], an algorithm is proposed to construct optimized networks related to a combination of local and global synchronization measures. Their objective function is computed and refined after successive numerical integrations. Although we follow a different approach, we point out that our results also support that “the early onset of synchronization and rapid transition to the phase-lock are conflicting demands on the network topology” [14]. Reference [15] associates a percolation process to the spread of synchronization. In addition, they consider node interchange in the graph based on a vertex-weighted graph measure. However, their characterization takes into account only the phase sign of neighbor oscillator. Even so, we also found a similar explosive synchronization.

It is common sense that a way to achieve more homogeneous neighborhood patterns is to gather members with closer intrinsic dynamics into communities. Thus, articles

<sup>\*</sup>cbnfreitas@gmail.com<sup>†</sup>elbert.macau@inpe.br<sup>‡</sup>viana@fisica.ufpr.br

that investigate this framework can also benefit from our findings. Reference [16] addresses a Kuramoto model of identical oscillators showing that, as the transient time dies out, synchronization occurs in stages matching the granular communities of the coupling graph. Reference [17] deals with communities of oscillators having essentially different natural frequencies. The authors of this paper discuss ways to promote or suppress synchrony on individual subgroups. Reference [18] introduces a dynamic feedback control to produce intracommunities synchronization regarding communities of identical nonlinear oscillators. Accordingly, Similar, Neutral, and Dissimilar patterns can be used as an additional tool to tune synchronization properties.

## II. MODEL AND METRICS

We consider a system of  $N$  phase oscillators, whose dynamics for the  $i$ th oscillator is

$$\dot{\theta}_i = \mathcal{W}_i + \frac{\varepsilon}{d_i} \sum_{j=1}^N A_{ij} \sin \theta_j - \theta_i, \quad (1)$$

where  $\mathcal{W} = \mathcal{W}_1, \dots, \mathcal{W}_N \in \mathbb{R}^N$  are the oscillator's *natural frequencies*. We consider  $\mathcal{W}$  with zero mean [19], randomly drawn from the uniform distribution over  $[-\pi, \pi]$ . A single choice of  $\mathcal{W}$  is drawn for each network size  $N$  studied.

The *coupling strength*  $\varepsilon \geq 0$  is the system parameter that adjusts the intensity of attractiveness between neighbor oscillators. The symmetrical *coupling graph* is expressed by its adjacency  $N \times N$  matrix  $A$ , so  $A_{ii} = 0$ ;  $A_{ij} = 1$  if oscillators  $i, j$  are neighbors (adjacent), and  $A_{ij} = 0$  otherwise. We assume connected graphs, meaning that there is a sequence of edges joining any two vertexes in the graph. Also,  $d_i := \sum_j A_{ij}$  stands for the  $i$ th vertex degree. The Laplacian matrix is defined as  $L := \text{diag } d_1, \dots, d_N - A$  and its eigenvalues are  $0 = \lambda_1 \leq \lambda_2 \leq \dots \leq \lambda_N$ . The first nontrivial eigenvalue  $\lambda_2$ , the *algebraic connectivity*, is greater than zero if and only if the graph is connected [20].

On one hand, analytical results [21] guarantee convergence to a unique (modulus  $2\pi$ ) stable phase-locked regime, where phase differences between every two oscillators becomes constant. Precisely, this convergence occurs if the coupling strength  $\varepsilon$  is large enough in comparison with  $\|\mathcal{W}\| \lambda_N / \lambda_2^2$ , where  $\|\cdot\|$  denotes the Euclidean norm in  $\mathbb{R}^N$ . Because  $\lambda_2$  increases when the graph diameter  $D$  is decreased and  $\lambda_N$  decreases with its maximum degree  $d_{\max}$  [22], phase locking can be achieved for smaller values of  $\varepsilon$  mostly with the reduction of  $D$  but also with smaller values of  $\|\mathcal{W}\|$  and  $d_{\max}$ . On the other hand, if we consider a system with only two phase oscillators, then it is well known [6] that the relation between its dissonance  $\nu := \mathcal{W}_1 - \mathcal{W}_2$  versus the coupling strength  $\varepsilon$  determines the synchronization regime [23]. So we introduce the *total dissonance* measure for vertex-weighted graphs as

$$\nu_{\text{Total}} := \frac{1}{N} \sqrt{\sum_{i,j=1}^N A_{ij} \mathcal{W}_i - \mathcal{W}_j^2}. \quad (2)$$

Since we consider symmetrical and connected coupling graphs, it is straightforward to check that  $\nu_{\text{Total}} = 0$  if and

only if all oscillator are identical. If we write  $\nu_{\text{Total}} = \nu_{\text{Total}} \mathcal{W}$ , then this measure quantifies how far  $\mathcal{W}$  is from a condition where all natural frequencies are identical. Therefore,  $\nu_{\text{Total}}$  encompasses information about the total spreading of  $\mathcal{W}$  by summing up individual dissonances over the coupling graph edges.

The norm of the global mean field, the *order parameter*, will be denoted by  $R\theta = |1/N \sum_{i=1}^N e^{i\theta_i}|$ . This quantity  $R$  ranges from 0 to 1, respectively, indicating that the ensemble gradually changes from null global mean field, where all phasors  $e^{i\theta_i}$  cancel out, to full synchronization, where  $\theta_1 = \dots = \theta_N$ . One also makes use of the *edge partial synchronization index* between two oscillators  $i, j$ ,

$$S_{ij} = S_{ji} := \left| \lim_{\Delta t \rightarrow \infty} \frac{1}{\Delta t} \int t_r t_r + \Delta t e^{i[\theta_i t - \theta_j t] t} \right|,$$

where  $t_r$  is a large enough transient time [24]. Oscillators  $i, j$  are phase locked, that is,  $\theta_i t - \theta_j t$  converges to a constant value if and only if  $S_{ij} = 1$ . Moreover, if this index is decreased towards zero, then weaker forms of synchronization and later uncorrelated trajectories occur [25]. We average contributions of all neighbor oscillators in the network to define the *partial synchronization index*

$$S := \frac{1}{\tilde{E}} \sum_{i,j=1}^N A_{ij} S_{ij}, \quad (3)$$

where  $\tilde{E} := \sum_{i,j=1}^N A_{ij}$  is the quantity of directed edges in the graph. Of course, the number of undirected edges is  $E := \tilde{E}/2$ . Thus,  $S = 1$  means that the whole ensemble is phase locked, while  $S \approx 0$  yields very low coherent ensemble behavior. Note that  $R[\theta t]$  converges to a constant value [26] if and only if  $S = 1$ .

An Adams-Bashforth-Moulton method for numerical integration is applied. A transient time of at least  $2 \times 10^3$  units of time was suppressed from the data, while the convergence of approximations of  $S$  over successive time windows of  $10^3$  units of time was the criterion to interrupt the integration. The mean value of  $R[\theta(t)]$  after the transient is denoted by  $\langle R \rangle$ . For a given choice of parameters and initial conditions, we indicate by  $\varepsilon_{\text{PL}}$  the smallest critical coupling strength  $\varepsilon > 0$  inducing phase locking, i.e.,  $S = 1$  and  $R[\theta t]$  converges to a constant value, which we denote by  $R_{\text{PL}}$ .

Several complex networks topologies [11] with  $N$  nodes and  $E$  (undirected) edges are considered: 4-Regular ( $N$  RE), Barabási-Albert ( $N$  BA), Erdős-Rényi ( $N$  ER), and Watts-Strogatz [27] ( $N$  WS). Experiments with relatively small networks with  $N = 50$  are performed for the sake of easy visualization. Larger ones, with  $N = 500$ , are also addressed to illustrate graphs closer to the theoretical degree distribution [11], yet feasible to massive numerical integration. To diminish computational cost and to allow comparison among network topologies, we consider graphs with  $\tilde{E} = 4N$  directed edges, which yields mean node degree  $\langle d \rangle = \tilde{E}/N = 4$ .

An empirical example of complex network with community structure, denoted by 105 CO, is included in the simulations: the Krebs-Amazon Political Books network [28]. This graph

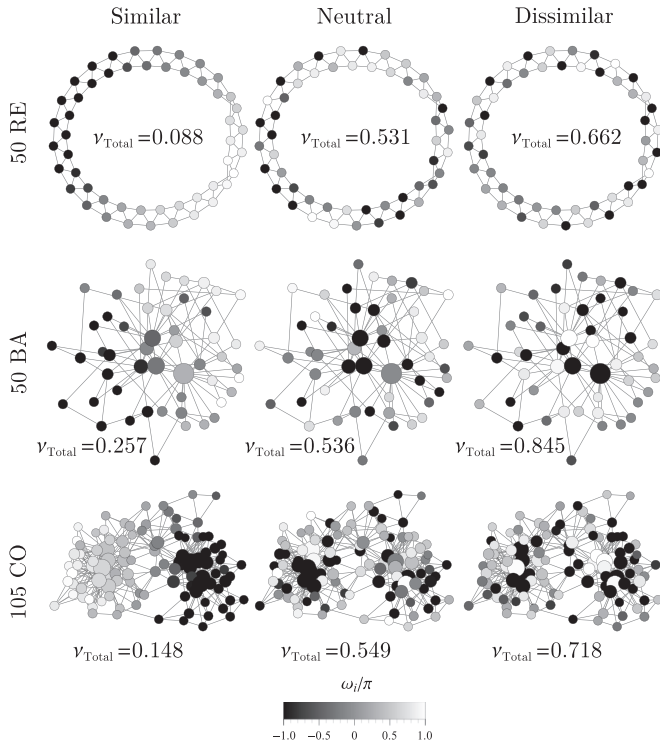


FIG. 1. Examples of Similar, Neutral, and Dissimilar patterns related to  $N$ -node graphs following network topology: 4-Regular ( $N$  RE); Barabási-Albert ( $N$  BA), with  $E = 100$  edges and a community graph ( $N$  CO) with  $E = 441$ . Vertex color is presented according to its natural frequency  $\mathcal{W}_i$ , ranging from  $-\pi$  (black) to  $\pi$  (white); vertex size is proportional to node degree. The associate total dissonance  $\nu_{\text{Total}}$  is displayed.

comprises  $N = 105$  nodes,  $\tilde{E} = 882$  edges, and two communities.

Our aim now is to make precise the subjective idea of Similar, Neutral, and Dissimilar patterns based on member's local choice of neighbors. Only oscillator swapping among the graph nodes are taken into account. Similar patterns should place oscillators alike into adjacent graph nodes. Thus, a way to achieve it for RE networks is to assign extreme natural frequency values, close to  $\pm\pi$ , as far as possible in the graph, filling intermediate nodes with gradual values of  $\mathcal{W}_i$ ; see Fig. 1 (50 RE Similar).

To consolidate this concept for more general network topologies, a numerical procedure is chosen as a definition. We will call the Similar configuration the permutation obtained by minimizing the objective function  $\nu_{\text{Total}}\mathcal{W}$ , which corresponds to minimize the dissonance  $\mathcal{W}_i - \mathcal{W}_j$  over all edges  $i, j$  of the graph. In contradistinction, Dissimilar configurations will be associated with maximization of the total dissonance. For this purpose, a simulated annealing optimization method (SA) [29] is employed to track permutations of  $\mathcal{W}$  towards optimal solutions [30].

The reader must be aware that although the SA returns permutations enhancing the objective function value, this is a stochastic scheme, which means that only with infinite iterations one could expect to achieve the global optima regarding all  $N!$  permutations. Nevertheless, whether these

numerical approximations of the total dissonance  $\nu_{\text{Total}}\mathcal{W}$  values are the global extremes values is not strictly relevant to our analysis.

Medium to large networks with a quantity of edges much smaller than the fully coupled case are the focus of the present study. Therefore, an initial random assignment of  $\mathcal{W}$  into the graph nodes, without any optimization process, will be called a neutral configuration. We take this approach by simplicity, because the total number of permutations  $N!$  becomes so massive that the probability of randomly drawing a permutation such that  $\nu_{\text{Total}}$  is close to the extreme values is very small, as is numerically confirmed below.

In conclusion, we derive from each pair  $A, \mathcal{W}$  the Neutral configuration, without optimization, and the Similar and Dissimilar ones by means of numerical minimization and maximization of  $\nu_{\text{Total}}\mathcal{W}$  [31], respectively. We defer to future research the study of other values of this metric, between Similar-Neutral and Neutral-Dissimilar, versus synchronization features.

Figure 1 illustrates RE, BA, and CO graphs with the three neighborhood patterns. As expected, from the RE graph with Similar configuration of this figure, one realizes a homogeneous transition of  $\mathcal{W}_i$  values. Each node presents indeed natural frequency close to the respective average of its neighbors. However, this ordering arises differently depending on the network topology. Hubs of the BA graph were colored with medium gray tones, corresponding to the overall mean of natural frequency distribution. But in the CO graph, positive and negative natural frequency values were placed into distinct communities, with hubs close to  $\pm\pi/2$  and central nodes (in between communities) close to null  $\mathcal{W}_i$ .

Regarding the Dissimilar configurations from Fig. 1, the opposite organization is found: each node receives natural frequency far from its neighbors. For the RE network, we notice sequences of connected nodes with alternating positive and negatives values of  $\mathcal{W}_i$ . Moreover, BA and CO graphs presented connected hubs with larger natural frequencies and opposite signs. Eventually, the Neutral configuration can be regarded as a blending between both previous configurations.

We randomly generate and include in our experiments 100 graphs of BA, ER, and WS network topologies in the next experiments. Since RE topology is deterministic and the CO graph was extracted from a data set, these classes contain a single member to be analyzed.

Figure 2 displays a distribution chart of the total dissonances  $\nu_{\text{Total}}$  obtained for the categories included in this article. From this figure, a sharp distinction among patterns is noticed, since there is no  $\nu_{\text{Total}}$  range overlapping within each category. Although this three-cluster structure arose from our data dealing with a variety of networks, it depends on the network size, topology, and suitable optimization algorithm. For instance, if the optimization output were not sufficiently far from the mean of the total dissonance distribution, then these patterns would have no meaning.

The set of graphs with  $N = 500$  presented values of  $\nu_{\text{Total}}$  3 times smaller than the set with  $N = 50$ . Furthermore, both sets were qualitatively alike, which is an evidence that we were capable to produce Similar and Dissimilar neighborhoods in the large networks, at least as well as the small ones.

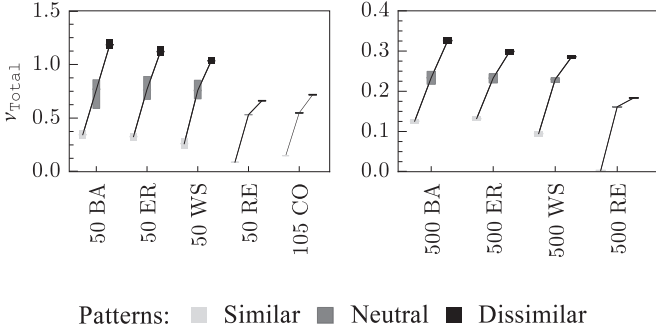


FIG. 2. Total Dissonance  $\nu_{\text{Total}}$  distribution chart of different topologies with Similar (light gray), Neutral (gray), and Dissimilar (black) patterns. Data correspond to the single members from categories 50 RE, 500 RE, and 105 CO and 100 different elements for the others. Colored bars indicate the overall range of  $\nu_{\text{Total}}$  obtained, while mean values of each distribution are joined by a black line within each category.

Because there is only a normalization by the number of vertices in the graph, but not by the quantity of edges, in Eq. (2), the total dissonance decreases with smaller mean degrees in all categories as expected [32]. BA, ER, and WS topologies were almost indistinguishable in the Neutral pattern but were slightly higher in this order for the Dissimilar case. All patterns of 50 RE and 105 CO graphs yielded smaller but comparable with each other total dissonance values.

We use notation and also denote by  $S$ ,  $\langle R \rangle$ ,  $\varepsilon_{\text{PL}}$ , and  $R_{\text{PL}}$  the associated mean values of these synchronization quantifiers considering all graphs of each category. A fixed random choice of initial condition  $\theta^0 \in \mathbb{R}^N$  is drawn from a uniform distribution over the unit circle for each network size  $N$ . So Fig. 3 displays the values of  $S$  and  $\langle R \rangle$ , as solid and dashed lines, respectively, obtained through numerical integration for the three neighborhood configurations colored like in Fig. 2. The time variable of both  $S$  and  $\langle R \rangle$  times series are rescaled to end at the associated mean critical coupling value  $\varepsilon_{\text{PL}}$ . The  $S$  lines finish at value 1, within the numerical tolerance, while

the final value of  $\langle R \rangle$  lines equal to the mean critical order parameter  $R_{\text{PL}}$ .

First, one focus on the phase-locking measures  $\varepsilon_{\text{PL}}$  and  $R_{\text{PL}}$ . Irrespective to network size, overall results were alike. In general,  $\varepsilon_{\text{PL}}$  decreases from Similar, Neutral, to Dissimilar patterns; while  $R_{\text{PL}}$  tend to increase in the same ordering. In all topologies, Similar cases demanded higher coupling strength to achieve phase locking. In particular, since this holds true even for RE networks, it shows that total dissonance patterns induce a different phenomenon than the ones from Refs. [12,13].

Moreover, even when these networks were phase locked,  $R$  converged to smaller values of  $R_{\text{PL}}$ . In other words, Similar ensembles tend to be harder to synchronize and to converge to regimes where oscillators were more spread around the unit circle than their counterparts. Neutral patterns required smaller  $\varepsilon_{\text{PL}}$  than Dissimilar ones. RE graphs were the only exception for these behavior of  $R_{\text{PL}}$ .

For all topologies, higher values of  $\varepsilon_{\text{PL}}$  were measured when  $N$  was multiplied by 10. On the other hand, larger networks yielded higher  $R_{\text{PL}}$  for Similar and Neutral neighborhoods but slightly smaller  $R_{\text{PL}}$  for Dissimilar ones.

At this point, the influence of Similar, Neutral, and Dissimilar patterns over the emergence of phase synchronization is investigated, especially related to coupling strengths  $\varepsilon$  much smaller than  $\varepsilon_{\text{PL}}$ .

Again, except for RE graphs, we verify that Similar patterns favor weaker synchronization regimes, since the initial growth of  $S$  and  $\langle R \rangle$  for small coupling strength  $\varepsilon$  is more prominent. However, beyond intermediate values of  $\varepsilon$ , Dissimilar patterns surpass the Similar ones through an abrupt transition. The Neutral case is between these two extremes, closer to the behavior of the Dissimilar group. If we compare network topologies, BA and ER graphs displayed close values of  $S$ , which were smaller than WS ones for small and intermediate values of  $\varepsilon$ .

A parallel of our findings could be made by considering conflicting ideas, associating communication and agreement with the emergence of synchronization and phaselocking,

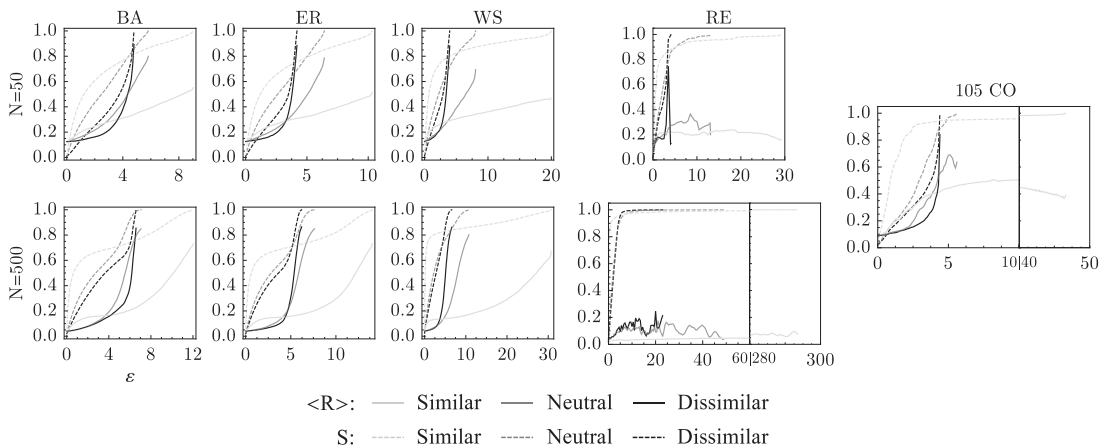


FIG. 3. Mean order parameter after transient  $\langle R \rangle$  and partial synchronization index  $S$ , solid and dashed lines respectively, as a function of coupling strength  $\varepsilon$  for different graph topologies. Average values of all graphs simulated within each category are shown. Similar, Neutral, and Dissimilar cases are respectively plotted in light gray, gray, and black. Lines are drawn to  $\varepsilon$  equal to the respective average critical phase locking  $\varepsilon_{\text{PL}}$ .

respectively. In Similar scenarios, interaction mostly occurs among people with closely related culture backgrounds. Thus, communication can easily spread locally, but the overall population, which contains diverse members, will hardly find a compromise. On the other hand, when networks contain more heterogeneous neighbors, as in the Neutral and Dissimilar cases, communication demands higher effort to be established. But after that, the whole ensemble is capable to rapidly reach consensus.

In summary, experiments with several network topologies were analyzed and a strong numerical trend was found. The Neutral case behaves in general between both extremes, closer to the Dissimilar case. Except for RE networks, under small coupling strength  $\varepsilon$ , Similar patterns yield larger values of

partial synchronization index  $S$ , meaning early synchronization ongoing. In contradistinction, Dissimilar ones present smaller values of  $S$  but undergo abrupt increment until phase locking. Moreover, all networks with Similar patterns required higher values of coupling strength to achieve phase locking, while Dissimilar patterns converged to regimes closer to full synchronization.

#### ACKNOWLEDGMENTS

We thank the Coordenação de Aperfeiçoamento de Pessoal de Nível Superior—CAPES (Process No. BEX 10571/13-2), CNPq, and FAPESP (Grant No. 2011/50151-0) for financial support.

- 
- [1] J. V. Hamm, *Dev. Psychol.* **36**(2), 209 (2000).
- [2] H. Abadzi, *J. Educ. Res.* **79**, 36 (1985).
- [3] T. B. Reusch, M. A. Haerberli, P. B. Aeschlimann, and M. Milinski, *Nature* **414**, 300 (2001).
- [4] C. Lozares, J. M. Verd, I. Cruz, and O. Barranco, *Qual. Quant.* **48**, 2657 (2014).
- [5] Y. Kuramoto, *Chemical Oscillations, Waves, and Turbulence*, Springer Series in Synergetics (Springer-Verlag, Berlin, 1984).
- [6] A. Pikovsky, M. Rosenblum, and J. Kurths, *Synchronization: A Universal Concept in Nonlinear Sciences*, Cambridge Nonlinear Science Series (Cambridge University Press, Cambridge, 2003).
- [7] S. H. Strogatz, *Nature* **410**, 268 (2001).
- [8] A. Arenas, A. Díaz-Guilera, J. Kurths, Y. Moreno, and C. Zhou, *Phys. Rep.* **469**, 93 (2008).
- [9] G. Filatrella, A. H. Nielsen, and N. F. Pedersen, *Eur. Phys. J. B* **61**, 485 (2008).
- [10] R. Follmann, E. E. N. Macau, E. Rosa, and J. R. C. Piqueira, *IEEE Transactions on Neural Networks and Learning Systems* **26**, 1539 (2015).
- [11] M. v. Steen, *Graph Theory and Complex Networks: An Introduction* (Maarten van Steen, Lexington, 2010).
- [12] J. Gómez-Gardeñes, S. Gómez, A. Arenas, and Y. Moreno, *Phys. Rev. Lett.* **106**, 128701 (2011).
- [13] P. Ji, Thomas K. D M. Peron, P. J. Menck, F. A. Rodrigues, and J. Kurths, *Phys. Rev. Lett.* **110**, 218701 (2013).
- [14] M. Brede, *Eur. Phys. J. B* **62**, 87 (2008).
- [15] X. Zhang, Y. Zou, S. Boccaletti, and Z. Liu, *Sci. Rep.* **4**, 5200 (2014).
- [16] A. Arenas, A. Díaz-Guilera, and C. J. Pérez-Vicente, *Phys. Rev. Lett.* **96**, 114102 (2006).
- [17] M. Komarov and A. Pikovsky, *Phys. Rev. Lett.* **110**, 134101 (2013).
- [18] K. Wang, X. Fu, and K. Li, *Chaos* **19**, 023106 (2009).
- [19] Without loss of generality, otherwise this mean value can be absorbed into the space stated and eliminated with a coordinate change.
- [20] C. Godsil and G. Royle, *Algebraic Graph Theory*, Graduate Texts in Mathematics, Vol. 207 (Springer-Verlag, New York, 2001).
- [21] A. Jadbabaie, N. Motee, and M. Barahona, in *Proceedings of the American Control Conference, 2004*, Vol. 5 (IEEE, New York, 2004), pp. 4296–4301.
- [22] J.-S. Li and X.-D. Zhang, *Linear Algebra Appl.* **285**, 305 (1998).
- [23] Arnold Tongues, for instance, can describe this interplay [6].
- [24] J. Gómez-Gardeñes, Y. Moreno, and A. Arenas, *Phys. Rev. Lett.* **98**, 034101 (2007).
- [25] C. B. N. Freitas, E. E. M. Macau, and R. L. Viana, in *Proceedings of the 22nd International Congress of Mechanical Engineering (Brazilian Association of Engineering and Mechanical Sciences, Ribeirão Preto, SP, Brazil, 2013)* pp. 10334–10339.
- [26] It is straightforward to check that this constant value cannot be the unit for nonidentical oscillators.
- [27] Watts-Strogatz networks with rewiring probability of 0.25 are considered.
- [28] Data-set description at <http://www.orgnet.com/> and adjacency matrix from <http://moreno.ss.uci.edu/data.html>.
- [29] S. Kirkpatrick, *J. Stat. Phys.* **34**, 975 (1984).
- [30] Actually, successive iterations of the SA using three strategies for node interchange are applied. First, nodes to be swapped are drawn with probability proportional to vertex degree, since they are the ones which influence the most  $\nu_{\text{Total}}$ . We also pick vertexes to be interchanged only within the same modularity-based community. Thus, we can focus the optimization process on relatively detached graph regions. Last, to facilitate escape from local critical points and also to fine adjustments, we consider all nodes equiprobable.
- [31] The essential purpose of the total dissonance  $\nu_{\text{Total}}$  in this work was to lay constructive foundation for Similar, Neutral, and Dissimilar configurations. One could reformulate these concepts based on variations of Eq. (2).
- [32] From the optimization point of view, the normalization by any constant value, whether the number of edges  $E$  or the quantity of nodes  $N$ , does not influence the Similar and Dissimilar configurations obtained. We opt not to normalize by  $E$  to reflect that the more edges a graph contains, the more conflicting pairs of dissonances exist in the network, which yields higher total dissonance.